Peak Systolic Mitral Annulus Velocity Reflects the Status of Ventricular-Arterial Coupling—Theoretical and Experimental Analyses

Kazunori Uemura, MD, PhD, Toru Kawada, MD, PhD, Kenji Sunagawa, MD, PhD, and Masaru Sugimachi, MD, PhD, *Suita and Fukuoka, Japan*

Background: Peak systolic mitral annular velocity (S_m) measured by tissue Doppler echocardiography has been recognized as an independent predictor of mortality in patients with heart failure and in the general population. However, the mechanical determinants of S_m remain poorly defined.

Methods: A theoretical model of S_m was derived, which indicates that S_m is affected positively by left ventricular (LV) contractility and preload and inversely by LV afterload and ejection time (EJT). In 16 anesthetized dogs, S_m, LV volume, and LV pressure were measured using sonomicrometry and catheter-tip micromanometry. LV contractility, preload, and afterload were indexed by the end-systolic pressure/volume ratio (E_{es}'), end-diastolic volume (V_{ed}), and effective arterial elastance (E_a), respectively. LV contractility, loading conditions, and heart rate were varied over wide ranges, and a total of 76 data sets were obtained for S_m (1.2–9.1 cm/sec), E_{es}' (1.5–17.6 mm Hg/mL), V_{ed} (11–99 mL), E_a (3.6–58.4 mm Hg/mL), EJT (100–246 msec), heart rate (66–192 beats/min), and the ventricular-arterial coupling ratio (E_{es}'/E_a; 0.2–3.0).

Results: The theoretical model accurately predicted S_m ($R^2 = 0.79$, $P < .0001$). By univariate analysis, S_m was correlated significantly with E_{es}' ($R^2 = 0.64$, $P < .0001$) and with the reciprocal of E_a ($R^2 = 0.49$, $P < .01$). V_{ed} and EJT did not affect S_m. E_{es}'/E_a was correlated strongly with S_m ($R^2 = 0.73$, $P < .0001$). E_{es}' and the reciprocal of E_a were not correlated with each other.

Conclusions: LV contractility and afterload independently determine S_m. The effects of LV preload and EJT on S_m might be small, even though they are theoretically associated with S_m. S_m strongly reflects the status of ventricular-arterial coupling. (J Am Soc Echocardiogr 2011;24:582-91.)

Keywords: Echocardiography, Heart failure, Hemodynamics, Mechanics

Left ventricular (LV) longitudinal shortening during ejection is reflected by systolic mitral annular velocity, which can be measured by tissue Doppler (TD) echocardiography in clinical practice.[1] Peak systolic mitral annular velocity (S_m) has been reported to be an index of global LV systolic function.[2,3] Measurement of S_m allows the detection of cardiac dysfunction more sensitively than the evaluation of other conventional LV function indexes, such as LV ejection fraction (LVEF).[4] S_m is a powerful prognosticator of mortality in patients with heart failure[5] and in the general population.[6] Although these previous studies have highlighted the clinical utility of S_m measurement, the mechanical determinants of S_m remain poorly defined.

S_m is correlated positively with LVEF in patients with cardiac diseases.[2] A recent animal study demonstrated that S_m is correlated with the maximum value of the time derivative of LV pressure (LVP) (LV dP/dt_{max}), an indicator of LV systolic function.[7] These findings suggest that LV contractility contributes significantly to S_m. However, the magnitudes of LVEF and dP/dt_{max} change in response to alteration in loading conditions, even if the intrinsic LV contractility is preserved.[8] Intriguingly, S_m and LV end-systolic elastance (E_{es}; a relatively load independent index of LV contractility) were found not to be correlated in patients with hypertension.[9] Henein *et al.*[10] assessed the effects of acute alterations in afterload on S_m during peripheral vascular surgery and reported that an increase in afterload by aortoiliac clamping decreased S_m. In contrast, in patients undergoing cardiac surgery, S_m was insensitive to changes in afterload after infusions of vasoactive agents.[11]

Whether and to what degree LV contractility and loading conditions independently affect S_m remain controversial. A more comprehensive approach is required to address this issue. The purpose of this study was to clarify the mechanisms that regulate the magnitude of S_m. To that end, we first derived the theoretical relationship between S_m and cardiovascular parameters describing LV contractility,

From the Department of Cardiovascular Dynamics, National Cerebral and Cardiovascular Center Research Institute, Suita, Japan (K.U., T.K., M.S.); and the Department of Cardiovascular Medicine, Kyushu University Graduate School of Medical Sciences, Fukuoka, Japan (K.S.).

This work was supported by a grant-in-aid for scientific research (C-20500404) from the Ministry of Education, Culture, Sports, Science and Technology and by the Intramural Research Fund (22-1-5) for Cardiovascular Diseases of the National Cerebral and Cardiovascular Center.

Reprint requests: Kazunori Uemura, MD, PhD, Department of Cardiovascular Dynamics, National Cerebral and Cardiovascular Center Research Institute, 5-7-1 Fujishirodai, Suita 565-8565, Japan (E-mail: *kuemura@ri.ncvc.go.jp*).

0894-7317/$36.00

doi:10.1016/j.echo.2011.01.010

Abbreviations

CV = Coefficient of variation

E_a = Effective arterial elastance

E_{es} = End-systolic elastance

EJT = Ejection time

HR = Heart rate

LV = Left ventricular

LVEF = Left ventricular ejection fraction

LVP = Left ventricular pressure

LVV = Left ventricular volume

P_{es} = End-systolic pressure

S_m = Peak systolic mitral annular velocity

S_{mTD} = Peak systolic myocardial velocity on tissue Doppler echocardiography

SV = Stroke volume

SVR = Systemic vascular resistance

TD = Tissue Doppler

V_{ed} = End-diastolic volume

V_{es} = End-systolic volume

afterload, and preload. Second, in canine experiments, we simultaneously acquired LVP, LV volume (LVV), and S_m using a catheter-tipped micromanometer and sonomicrometer, while varying LV contractility and loading conditions over wide ranges. We compared these experimental data with the theoretical predictions and evaluated the independent effects of the parameters on S_m.

METHODS

Theoretical Relationship Between S_m and Cardiovascular Parameters

We based our theoretical modeling on the LVP-LVV framework,[12] as shown in Figure 1. E_{es}, the slope of the relationship between end-systolic pressure (P_{es}) and end-systolic volume (V_{es}), is an index of LV contractility (Figure 1A). Effective arterial elastance, E_a, the slope of the relationship between P_{es} and stroke volume (SV), is an index of LV afterload.[13] The time-elastance curve of the left ventricle has a distinct waveform (Figure 1B).[14,15] The time-elastance curve during systole can be approximated to two straight lines, one for the isovolumic contraction phase and the other for the ejection phase (Figure 1B).[14,15] S_m is related to E_{es}, E_a, LV end-diastolic volume (V_{ed}) and ejection time (EJT) by the following formula:

$$S_m = \frac{\alpha}{3} \cdot \frac{E_{es}}{E_a} \cdot \frac{V_{ed}^{1/3}}{EJT}, \quad (1)$$

where α is a constant determined by the ratio of LV longitudinal to short-axis length. Details of the mathematical derivation of equation 1 are provided in the Appendix.

Animal Experiments

We used 22 adult mongrel dogs (both sexes; weight, 20–30 kg). The investigation conformed with the *Guide for the Care and Use of Laboratory Animals*.[16] All protocols were approved by the Animal Subjects Committee of the National Cerebral and Cardiovascular Center.

Experiment 1: Comparison of Mitral Annular Velocities Measured by Sonomicrometry and TD Echocardiography

Preparation. Six animals were used. After anesthesia was induced with sodium pentobarbital (25 mg/kg), the animals were intubated endotracheally and ventilated artificially. An appropriate level of anesthesia was maintained by continuous inhalation of 1.5% isoflurane. A sterile left lateral thoracotomy was performed, and the pericardium was opened. Three spheric sonomicrometer crystals (2 mm in diameter) were implanted in the subepicardium at the base (Figure 2A, points 1 and 2) and apex (Figure 2A, point 3) of the left ventricle. All wires were exteriorized through the back of the neck. The pericardium and chest wall were closed, and the animal was allowed to recover.

After the animals had fully recovered from the procedure (10–14 days after surgery), mitral annular velocities were measured by sonomicrometry and TD echocardiography. During measurements, the dogs were anesthetized and artificially ventilated and were laid in a sling. Surface electrocardiograms were recorded.

Mitral Annular Velocity Measurement by Sonomicrometry. To obtain LV dimensions, sonomicrometric signals were processed with a digital system (Sonolab, Sonometrics Corporation, London, Canada) while each crystal sent a signal to and received a signal from each of the other crystals. Analog signals of sonomicrometric LV dimensions and electrocardiography were digitized at 200 Hz and stored for offline analysis (Sonolab). The dimensions of the three sonomicrometer crystals were used to calculate the LV longitudinal length (L), which is the distance between the LV apex and the center of the base (Figure 2A). The time derivative of L (dL/dt) was used as instantaneous mitral annular velocity, and a positive velocity was reported to indicate shortening of L.[17] Peak dL/dt during LV systole was used as S_m.

Mitral Annular Velocity Measurement by TD Echocardiography. Transthoracic echocardiography was performed using an echocardiographic system equipped with a 6-MHz transducer (Artida; Toshiba Corporation, Tokyo, Japan). Mitral annular velocity was obtained with pulsed TD from the apical four-chamber view by placing a 2-mm-wide sample volume at the septal side of the mitral annulus (Figure 2B).[3] Peak systolic myocardial velocity (S_{mTD}) was obtained.[3,5]

Data Acquisition. All data were acquired at end-expiration. To avoid interference between sonomicrometry and TD echocardiography, we first recorded echocardiographic data for 10 sec and then sonomicrometric dimensions during the subsequent 10 sec. Doses of dobutamine (2, 4, 8, and 16 μg/kg/min) and propranolol (0.2 mg/kg) were administered intravenously to each dog to modulate LV inotropy. S_m and S_{mTD} were determined after administration of each dose.

Experiment 2: Effects of Cardiovascular Parameters on S_m

Preparation. Sixteen animals were used. Anesthesia and artificial ventilation were conducted as described above. A fluid-filled catheter (8Fr) was placed in the right femoral artery to measure systemic arterial pressure. The fluid-filled catheter was connected to a pressure transducer (DX-200; Nihon Kohden, Tokyo, Japan). After a median sternotomy, the heart was suspended in a pericardial cradle. A pair of pacing electrodes was fixed at the right atrial appendage for atrial pacing. A catheter-tipped micromanometer (PC-751; Millar Instruments, Houston, TX) was inserted via the LV apex to measure LVP. As depicted in Figure 3A, 10 sonomicrometer crystals were implanted in the subepicardium of the left ventricle and the right side of the interventricular septum to obtain LV dimensions. Surface electrocardiograms were recorded. After the instrumentation was completed, the pericardium was closed. All data acquisitions were done at end-expiration. Analog signals of arterial pressure, LVP,

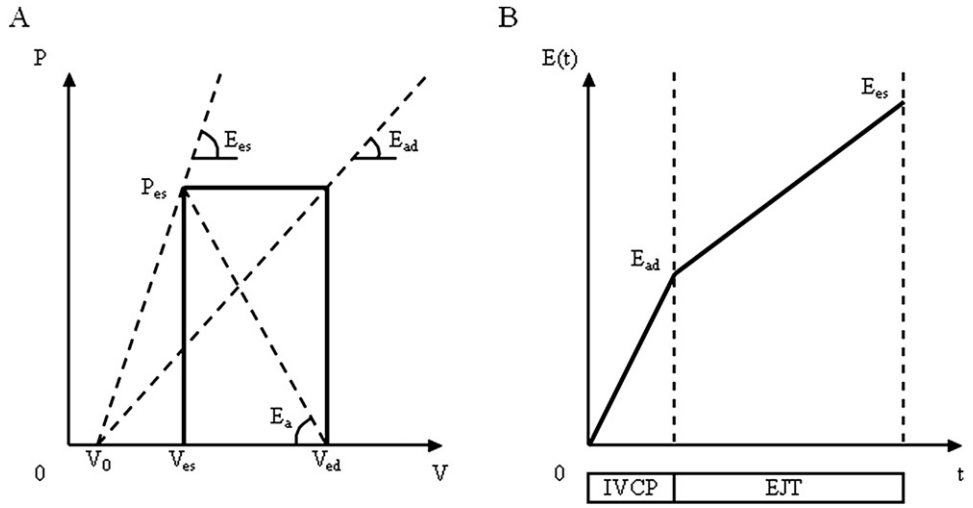

Figure 1 **(A)** Schematic drawing of the LVP (P)–LVV (V) loop, depicting E_{es}, E_{ad}, E_a, P_{es}, volume axis intercept of the relationship between P_{es} and V_{es} (V_0), V_{es}, and V_{ed}. **(B)** Bilinearly approximated time (*t*)–elastance (E[*t*]) curve during the isovolumic contraction phase (IVCP) and EJT.

sonomicrometric LV dimensions, and electrocardiography were digitized at 200 Hz and stored for offline analysis.

Experimental Protocols. After the initial preparation and surgical procedures were complete, the animals were allowed to stabilize for 30 min. Under steady-state baseline condition, we recorded the analog signals for about 10 sec in each animal. After obtaining the hemodynamic data at baseline conditions, we created various hemodynamic conditions, as described in the following protocols. In each protocol, we waited 20 min to confirm that hemodynamic conditions reached steady state.

*Contractility Run (*n = *9).*—Hemodynamic data were recorded while LV contractility was increased by dobutamine infusion (5 μg/kg/min). After the data were recorded, dobutamine infusion was temporarily suspended. We created acute heart failure by embolizing the left coronary artery with glass microspheres (90 μm in diameter). Data recording was repeated under depressed LV contractility. Hemodynamic data were also recorded after LV contractility was restored by reinfusion of dobutamine.

*Loading Run (*n = *7).*—Hemodynamic data were recorded after pharmacologically altering vascular resistance (afterload) and LV filling (preload) by infusing norepinephrine (0.2 μg/kg/min), sodium nitroprusside (3 μg/kg/min), or 250 mL of 10% dextran 40.

*Heart Rate (HR) Run (*n = *6).*—The possible dependence of S_m on HR was tested by suppressing the intrinsic atrial beat using zatebradine (UL-FS49; 0.5 mg/kg) and instituting atrial pacing to obtain hemodynamic data at different HRs (±25% of baseline HR).

Six animals underwent both loading and HR runs. At the conclusion of the experiments, the dogs were sacrificed with an intravenous injection of pentobarbital and potassium chloride. Autopsies were performed to verify the position of the sonomicrometer crystals and catheters. After excision of the adjacent right ventricular muscle, valvular tissue and fat, LV myocardial volume was measured by water displacement in a volumetric cylinder.

Data Analysis and Definitions. *Calculation of S_m.*—Dimensions between the sonomicrometer crystals placed at the LV base (Figure 3A, points 1 and 2) and the LV apex (Figure 3A, point 3) were used to calculate S_m, as described above.

LVV Calculation Using Sonomicrometric LV Dimensions.—The three-dimensional position of each crystal was defined as a function of time on the basis of the distances between the crystals.[18] The LV epicardial volume (including LVV and LV myocardial volume) was estimated using software that applied an ellipsoidal shell model to the coordinates of all 10 crystals (Figure 3A).[19] LVV was obtained by subtracting LV myocardial volume from the estimated LV epicardial volume. Our preliminary study demonstrated that ex vivo LVV thus estimated agreed reasonably well with the volume measured by intraventricular balloon method (LVV_{ba}) in four canine hearts ($LVV = 1.0 \times LVV_{ba} - 7.0$; $r = 0.98$; SEE = 14 mL; $20 \le LVV_{ba} \le 70$ mL).

Cardiovascular Parameters.—End-systole was defined as the time when LV dP/dt decreased to 20% of its minimum.[15] LV contractility was indexed by the P_{es}/V_{es} ratio ($E_{es}' = P_{es}/V_{es}$), which is an approximation of E_{es}.[9,20] V_{ed} (an index of LV preload) was defined as LVV at the peak of the R wave on the electrocardiogram.[11] E_a (an index of LV afterload) was defined as the ratio of P_{es} to SV ($SV = V_{ed} - V_{es}$).[9,13] The end of the isovolumic contraction phase was defined as the moment when LV dP/dt decreased to 80% of its maximum, according to a previous study[21] with minor modification. EJT was obtained by subtracting the end of the isovolumic contraction phase from end-systole. Systemic vascular resistance (SVR) was defined as time-averaged arterial pressure divided by the product of SV and HR. A previous study demonstrated that E_a is related to SVR and HR as follows: $E_a \approx k \times SVR \times HR$, where k is a constant.[13] The E_{es}'/E_a ratio was used as an index of ventricular-arterial coupling.[14,20]

S_m and cardiovascular parameters were the averages of approximately 10 beats.

Statistical Analysis

All data are presented as mean ± SD. Statistical analyses were performed using commercially available software (Statistica; Statsoft, Inc., Tulsa, OK). In experiments 1 and 2, the associations among variables were analyzed using a mixed-model procedure to handle the dependencies in repeated measurements within the same animal.[7,17,22,23] The coefficient of determination (R^2) was used to evaluate the strength of association, because it measures how much variability of the dependent variable is the result of the independent

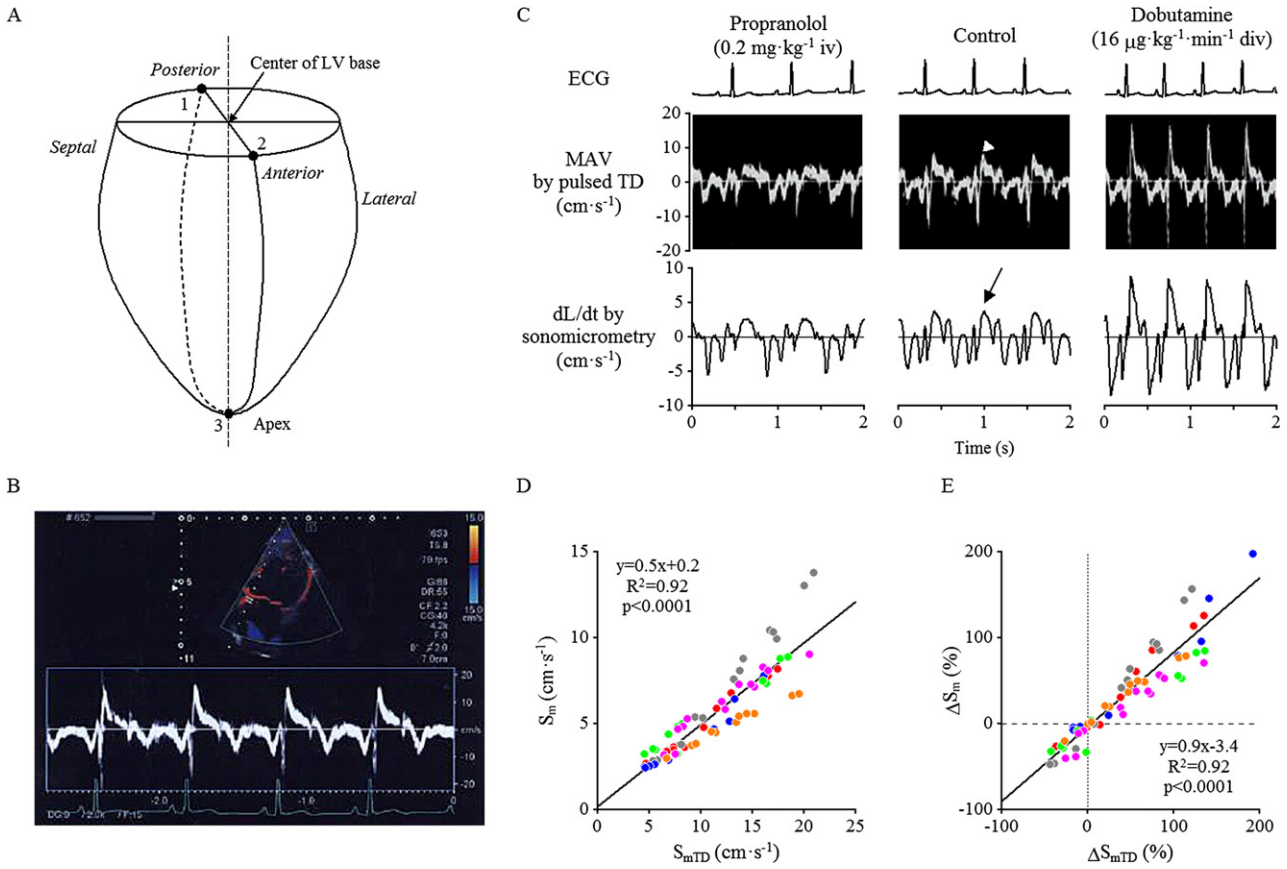

Figure 2 **(A)** Placement of sonomicrometer crystals (see text) in experiment 1. **(B)** Measurement of mitral annular velocity (MAV) at the septal side of the mitral annulus by TD echocardiography. **(C)** Examples of waveform data of electrocardiogram, septal MAV obtained from TD echocardiography, and dL/dt measured by implanted sonomicrometer crystals during hemodynamic alterations induced by dobutamine and propranolol. Data for dL/dt were traced so that positive values indicated shortening of LV longitudinal length.[17] Because of interference between sonomicrometry and Doppler, TD velocities were not from the same heartbeat as the other recordings. *Arrowhead*, S_{mTD}; *arrow*, S_m. **(D)** Relation between S_m and S_{mTD} in six dogs. Each *color* indicates the data from one animal. The line represents the population-averaged regression[20] between S_m and S_{mTD} with regression equation, coefficient of determination (R^2), and probability value. **(E)** Relation between percentage changes in S_m (ΔS_m) and S_{mTD} (ΔS_{mTD}) from their respective baseline values in six dogs. Each color indicates the data from one animal. The *line* represents the population-averaged regression between ΔS_m and ΔS_{mTD} with regression equation, R^2, and probability value.

variable.[7] In experiment 2, the coefficient of variation (CV) was calculated as the ratio of the SD to the mean (reported as a percentage) and used to quantify the variability of measurements. One-way repeated-measures analyses of variance with Dunnett's test were used in multiple comparisons relative to baseline for each intervention. P values $< .05$ were considered statistically significant.

RESULTS

Experiment 1: Mitral Annular Velocity Measured by Sonomicrometry and TD Echocardiography

Figure 2C displays representative recordings of mitral annular velocity measured by TD echocardiography and dL/dt measured by sonomicrometry when LV contractility was pharmacologically modulated. Waveforms derived from TD echocardiography were slightly different from those derived from sonomicrometry. As shown in Figure 2D, the values of S_{mTD} were consistently larger than those of S_m, but the two were correlated strongly on the basis of the data obtained from six canine hearts over a wide range of LV inotropy ($R^2 = 0.92$). Percentage change in S_{mTD} was also correlated highly with percentage change in S_m ($R^2 = 0.92$; Figure 2E). On the basis of these findings, instead of S_{mTD}, we used S_m by sonomicrometry to investigate the mechanical determinants of systolic mitral annular velocity, because this allowed analyses of all variables, including LVP and LVV, from the same heartbeat.

Experiment 2: Effects of Cardiovascular Parameters on S_m

Figure 3B shows traces of hemodynamic variables in one animal under baseline conditions. As predicted in our theoretical analysis (Appendix), S_m was detected early in the ejection phase.

Effects of Various Interventions on S_m and Cardiovascular Parameters. Table 1 summarizes the effects of various interventions on S_m and cardiovascular parameters (a total of 76 data sets). The CVs for S_m, E_{es}', V_{ed}, E_a, EJT, SVR, HR, and E_{es}'/E_a were 44%, 49%, 41%, 77%, 24%, 77%, 21%, and 64%, respectively. S_m and all the cardiovascular parameters changed over reasonably wide ranges by the interventions.

Contractility Run.—S_m, E_{es}', and E_{es}'/E_a changed in a similar pattern from their respective baseline values. They increased significantly with

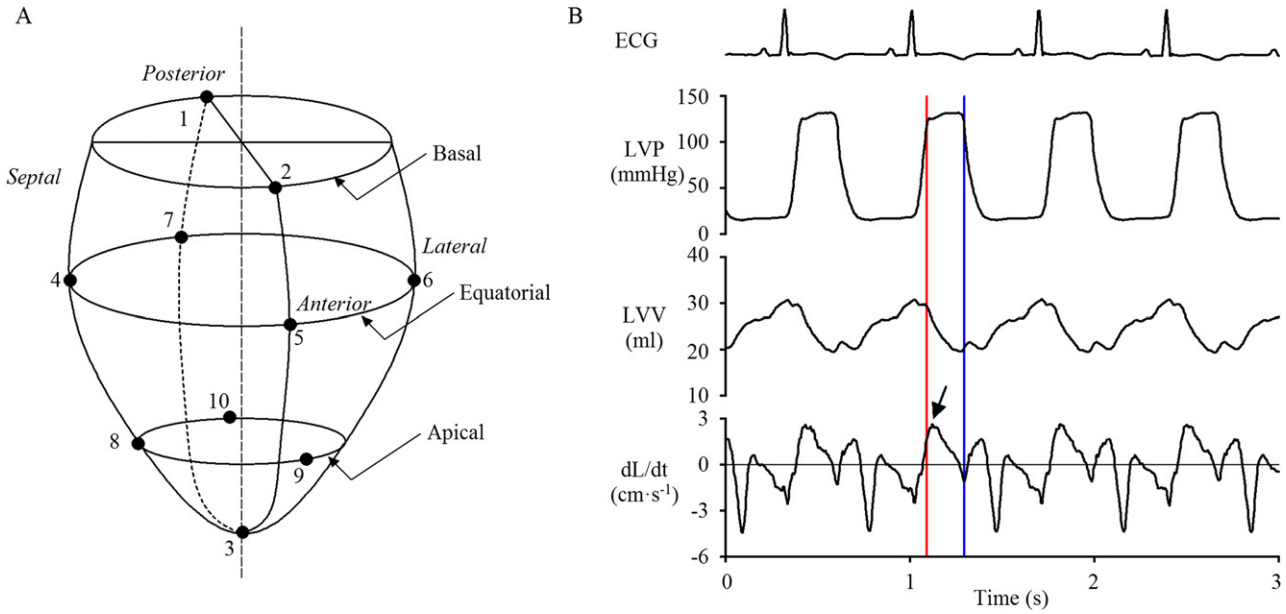

Figure 3 **(A)** Placement of sonomicrometer crystals (see text) in experiment 2. **(B)** Representative tracings from a dog in baseline condition. *Vertical red line*, end of isovolumic contraction phase; *vertical blue line*, end-systole; *arrow*, S_m.

dobutamine infusion, decreased significantly after acute heart failure induction, and recovered to baseline levels with reinfusion of dobutamine. V_{ed} and E_a significantly increased and EJT significantly decreased from their respective baseline values after acute heart failure induction.

Loading Run.—S_m, E_{es}', and E_{es}'/E_a did not change significantly in response to changes in loading conditions. Norepinephrine infusion significantly increased E_a and SVR and significantly decreased HR. Sodium nitroprusside infusion significantly decreased V_{ed} but did not significantly reduce E_a and SVR. Dextran infusion significantly increased V_{ed} and EJT and significantly decreased E_a and HR.

HR Run.—Zatebradine infusion significantly decreased HR and E_{es}' and significantly increased V_{ed} and EJT. Atrial tachypacing significantly increased HR. E_a was apparently decreased by zatebradine and increased by atrial tachypacing, although the differences were not significant.

Relationships Between S_m and Cardiovascular Parameters. Using the 76 data sets from all interventions, we examined whether S_m was related to the cardiovascular parameters as predicted by equation 1. As shown in Figure 4A, S_m was correlated significantly with the product of E_{es}' and the cubic root of V_{ed} divided by E_a and EJT. The R^2 value was 0.79, indicating that the theoretical model accurately predicts S_m.

Figures 4B to 4H shows univariate relationships between S_m and each of the cardiovascular parameters. S_m was correlated significantly with E_{es}' (Figure 4B). In accordance with equation 1, we related S_m with the cubic root of V_{ed} ($V_{ed}^{1/3}$; Figure 4C), with the reciprocal of E_a (E_a^{-1}; Figure 4D), and with the reciprocal of EJT (EJT^{-1}; Figure 4E). The CVs for E_a^{-1}, $V_{ed}^{1/3}$, and EJT^{-1} were 41%, 14%, and 21%, respectively. S_m was correlated significantly with E_a^{-1} but not with $V_{ed}^{1/3}$ and EJT^{-1}. Because E_a was correlated linearly with the product of SVR and HR, as described above, we related S_m with the reciprocal of SVR (SVR^{-1}; Figure 4F) and with the reciprocal of HR (HR^{-1}; Figure 4G). S_m was correlated significantly with SVR^{-1} but not with HR^{-1}. Figure 4H indicates that E_{es}'/E_a was tightly correlated with S_m.

We analyzed the correlations between the cardiovascular parameters. E_{es}' was not correlated with E_a^{-1} ($P=.96$), indicating that the two affect S_m independently. E_{es}' was correlated inversely with $V_{ed}^{1/3}$ ($E_{es}' = -4.3 \times V_{ed}^{1/3} + 21.7$; $R^2 = 0.56$, $P < .001$). E_a^{-1} was correlated inversely with EJT^{-1} ($E_a^{-1} = -0.03 \times EJT^{-1} + 0.34$; $R^2 = 0.76$, $P < .0001$). E_a^{-1} was correlated positively with $V_{ed}^{1/3}$ ($E_a^{-1} = 0.05 \times V_{ed}^{1/3} + 0.03$; $R^2 = 0.68$, $P < .01$). $V_{ed}^{1/3}$ was correlated inversely with EJT^{-1} ($V_{ed}^{1/3} = -0.16 \times EJT^{-1} + 4.45$; $R^2 = 0.76$, $P < .001$).

DISCUSSION

To the best of our knowledge, this is the first study to comprehensively evaluate the relations between S_m and cardiovascular parameters using theoretical modeling and also well-controlled animal experiments. The theoretical model of S_m indicates that S_m is affected by LV contractility, preload, afterload, and EJT. Experimental data confirmed that the theoretical model accurately predicts S_m. Further analysis of the experimental data showed that LV contractility and afterload have independent effects on S_m, but LV preload and EJT do not. S_m strongly reflects the status of ventricular-arterial coupling.

Mechanical Determinants of S_m

The theoretical model of S_m is rational mechanically because the right side of equation 1 corresponds to the mean velocity of LV shortening. The product of E_{es}/E_a and V_{ed} positively correlates with SV.[13] Therefore, the product of E_{es}/E_a and the cubic root of V_{ed}, which corresponds to LV end-diastolic dimension, positively correlates with the stroke dimension of the left ventricle. The stroke dimension of the left ventricle divided by EJT equals the mean velocity of LV shortening.

In our theoretical analysis, we assumed that changes in LV length couple with changes in LVV (Appendix). Actually, this is not the case throughout the cardiac cycle. In the isovolumic contraction

Table 1 Effect of interventions on systolic mitral annular velocity and cardiovascular parameters

Variable	S_m (cm/sec) 3.3 ± 1.5 (1.2–9.1)	E_{es}' (mm Hg/mL) 7.5 ± 3.7 (1.5–17.6)	V_{ed} (mL) 37 ± 16 (11–99)	E_a (mm Hg/mL) 9.2 ± 7.1 (3.6–58.4)	EJT (msec) 150 ± 36 (100–246)	SVR (mm Hg/sec/mL) 4.4 ± 3.3 (1.3–21.4)	HR (beats/min) 130 ± 28 (66–192)	E_{es}'/E_a 1.0 ± 0.7 (0.2–3.0)	*n* 76
Contractility run									
Baseline	3.4 ± 1.2	6.2 ± 1.7	38 ± 9	6.7 ± 1.4	134 ± 12	2.9 ± 0.7	130 ± 11	1.0 ± 0.4	9
DOB	6.0 ± 1.8†	10.5 ± 3.7†	45 ± 5	6.1 ± 1.6	127 ± 8	2.7 ± 1.1	136 ± 24	1.9 ± 0.9†	9
AHF	2.2 ± 1.0*	2.7 ± 0.8†	50 ± 17†	8.4 ± 2.4*	121 ± 13†	3.2 ± 1.0	145 ± 12	0.3 ± 0.1*	9
AHF with DOB	3.5 ± 0.9	4.3 ± 1.4	56 ± 17†	7.4 ± 1.3	117 ± 6†	2.8 ± 0.8	156 ± 26†	0.6 ± 0.1	9
Loading run									
Baseline	2.9 ± 0.7	9.3 ± 3.2	24 ± 7	10.6 ± 4.5	161 ± 21	5.2 ± 2.4	127 ± 19	1.1 ± 0.7	7
NE	2.8 ± 0.6	10.9 ± 3.9	29 ± 9	14.8 ± 7.9†	165 ± 25	9.0 ± 5.4†	103 ± 24†	0.9 ± 0.4	7
SNP	3.1 ± 0.6	9.5 ± 3.6	19 ± 6*	9.1 ± 4.3	158 ± 31	4.6 ± 2.0	127 ± 17	1.3 ± 0.8	7
DEX	3.1 ± 0.9	7.2 ± 1.6	39 ± 10†	7.1 ± 3.5*	209 ± 26†	3.9 ± 1.9	107 ± 14*	1.2 ± 0.5	7
Heart rate run									
Baseline	2.8 ± 0.7	9.9 ± 3.0	24 ± 7	10.5 ± 5.0	155 ± 16	4.8 ± 2.3	134 ± 8	1.1 ± 0.7	6
ZAT	2.9 ± 1.1	6.9 ± 1.0*	39 ± 9†	6.6 ± 3.0	204 ± 33†	4.5 ± 2.2	86 ± 4†	1.2 ± 0.4	6
PACE	3.0 ± 1.4	10.0 ± 2.7	22 ± 9	18.4 ± 19.9	143 ± 22	6.9 ± 7.3	165 ± 12†	0.9 ± 0.4	6

Data are shown as mean ± SD (range). Because there was an overlap in baseline parameters between the loading and heart rate runs, the sum of the numbers of all interventions was not 82, but 76.
AHF, Acute heart failure induced by coronary embolization; *DEX*, dextran infusion; *DOB*, dobutamine infusion; *NE*, norepinephrine infusion; *PACE*, atrial tachypacing; *SNP*, sodium nitroprusside infusion; *ZAT*, zatebradine infusion.
*$P < .05$.
†$P < .01$ versus baseline.

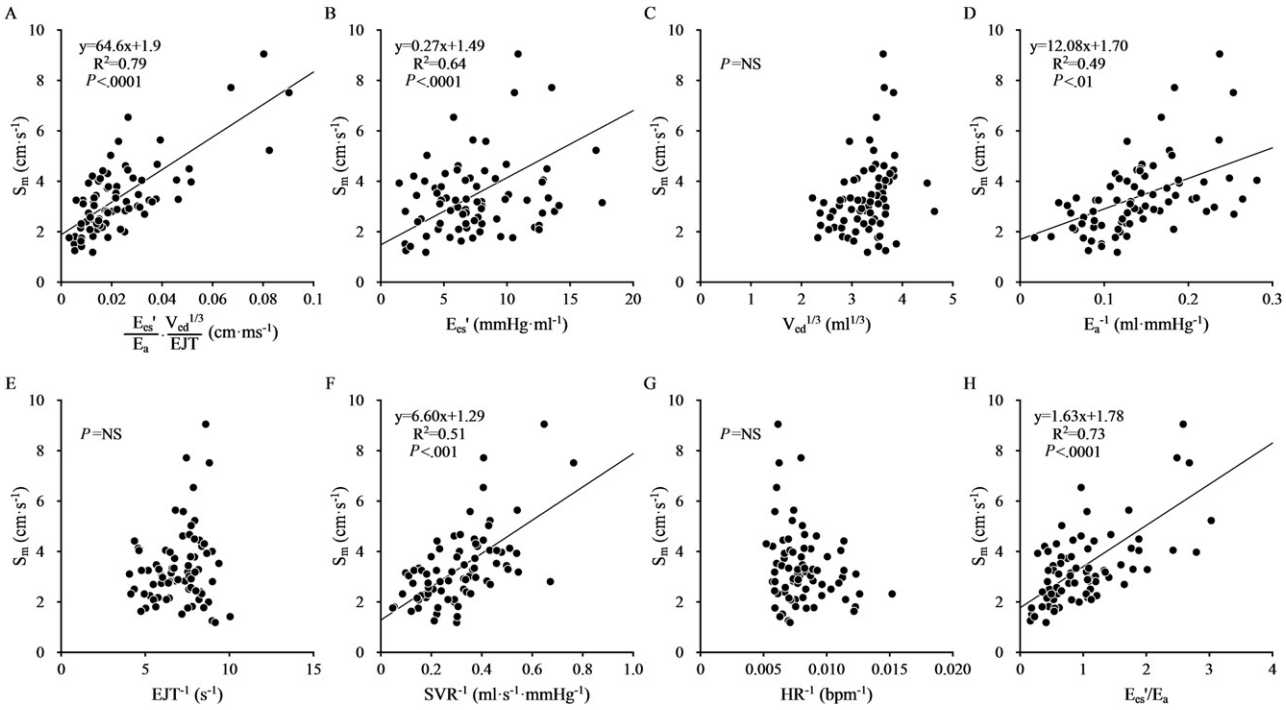

Figure 4 **(A)** Relationship between measured S_m and values obtained from the theoretical model consisting of the ratio of P_{es} to V_{es} (E_{es}'), V_{ed}, E_a, and EJT (see equation 1). **(B–H)** Relationships between S_m and E_{es}' **(B)**, the cubic root of V_{ed} **(C)**, the reciprocal of E_a **(D)**, the reciprocal of EJT **(E)**, the reciprocal of SVR **(F)**, the reciprocal of HR **(G)**, and the ventricular-arterial coupling ratio (E_{es}'/E_a) **(H)**. Each panel shows raw data from all interventions (76 data points) and the line representing the population-averaged regression between S_m and the cardiovascular parameters,[20] regression equation, R^2, and probability value.

phase, LV longitudinal and short-axis lengths change without change in LVV.[19] However, during the ejection phase, which was the phase of interest in our analysis, both LV longitudinal and short-axis lengths decreased in parallel with LVV. We also assumed that the ratio of LV longitudinal length to short-axis length is constant during the ejection phase (Appendix). The ratio is actually not constant. The ratio

averaged for eight dogs in a previous study was 1.65 at the beginning of the ejection phase.[19] At the end of the ejection phase, the ratio increased to 1.88. If these values are translated into α in equation 1, α increases from 1.73 to 1.89 (a net increase of 10%) during the ejection phase. Hence, α is actually not constant within one animal. Although this can be a confounder in this theoretical analysis (Appendix), its effect would be quantitatively small. Apart from α, the time-varying LV elastance, $E(t)$, also determines S_m (equation A9 in Appendix). If $E(t)$ is constant, S_m is achieved when α is maximum, that is, at the end of the ejection phase. Meanwhile, if α is constant, S_m is achieved when $E(t)$ is minimum, that is, at the beginning of the ejection phase. During the ejection phase, $E(t)$ increases from 5 to 10 mm Hg/mL in dogs (a net increase of 100%).[15] A numerical simulation using these published data indicates that the contribution of $E(t)$ to S_m is 15 times more than that of α. Thus, we can assume α as constant without sacrificing accuracy. S_m is effectively determined by $E(t)$ and is achieved at the beginning of the ejection phase. This is compatible with in vivo findings. In this study (Figures 2B, 2C, and 3B) and also in previous studies,[4,7,23] S_m is usually reached early in the ejection phase.

According to the value of R^2, the theoretical model can predict 79% of S_m variation. The residual variation, 21%, remains to be explained. Although it is possible that variation among animals of α in equation 1 may contribute to this residual variation, the CV of α in eight dogs was <5% in a previous study,[19] suggesting that variation among animals of α plays a minor role in the residual variation. The variation may be caused by factors not included in the model. A previous study indicated that dynamic arterial properties such as aortic compliance have direct effects on S_m.[10] Further studies to address these issues are required in the future.

LV contractility determines the magnitude of S_m. The R^2 value of 0.64 between S_m and E_{es}' in this study was comparable with those observed between S_m and other LV functional indexes, such as LV dP/dt_{max}, in previous studies.[7] Borlaug *et al.*[9] reported that S_m was not correlated with indexes of LV contractility including, E_{es}', in patients with hypertension. However, because they excluded patients with heart failure with depressed LV contractility from the study population and did not actively stimulate LV inotropy in their protocol, LV contractile indexes were well preserved with small variations among patients. This might be a reason they did not detect a significant correlation between S_m and indexes of LV contractility.

S_m is inversely related to LV afterload. Previous clinical studies have yielded contrasting results of dependence[9,10,24] and independence[11,25] of S_m on afterload. Oki *et al.*[24] reported that S_m was reduced in response to an increase in LV afterload after angiotensin infusion in healthy subjects. In contrast, Amà *et al.*[11] reported that S_m did not change when E_a and SVR were changed by phenylephrine or nitroglycerine infusion in patients undergoing cardiac surgery. However, they did not attempt to directly associate S_m with the afterload indexes. Similar to their results, we also noted that S_m did not change in response to phenylephrine infusion, whereas E_a or SVR significantly increased (Table 1). However, we further analyzed the associations between S_m and afterload indexes using mixed-model procedures. In the previous studies, conducting statistical analyses similar to those we performed in this study would have been useful to evaluate association between the afterload and S_m.

Unexpectedly, V_{ed} and EJT did not affect S_m independently. Both V_{ed} and EJT are components of our theoretical model of S_m. Furthermore, previous studies suggested that S_m was affected by LV preload and EJT.[23,26] In this study, the CVs for $V_{ed}^{1/3}$ and EJT^{-1} were small compared with those for E_{es}' and E_a^{-1}. Moreover, E_{es}' was correlated inversely with $V_{ed}^{1/3}$, and E_a^{-1} was correlated inversely with EJT^{-1}. These suggest that because of the low variability of $V_{ed}^{1/3}$ and EJT^{-1} and the antagonizing effects of the covariates (E_{es}' and E_a^{-1}), the analysis might fail to detect significant correlations of $V_{ed}^{1/3}$ and EJT^{-1} with S_m. However, V_{ed} also was not correlated with S_m in this study (data not shown), although the CVs for V_{ed} and E_{es}' were comparable (41% and 49%). It would be ideal to change V_{ed} or EJT individually while keeping all other parameters constant. Although impedance loading on ex vivo heart preparation would realize such protocols,[8] this preparation is inappropriate for the study of LV longitudinal function, because it requires resection of the mitral valve and subvalvular apparatus (papillary muscles), which are critical components of longitudinal function.[27] Taken together, although we cannot completely exclude significant contributions of LV preload and EJT to S_m, their effects may be small and easily reversed by the effects of LV contractility and afterload, that is, effectively negligible compared with the status of ventricular-arterial coupling.

Potential Clinical Implications

A novel and important finding of this study is that S_m strongly reflects the status of ventricular-arterial coupling. Ventricular-arterial coupling is a central determinant of cardiovascular performance and cardiac energetics.[13-15,28,29] Normally, the left ventricle and the arterial system are optimally coupled to produce maximal stroke work, when E_{es}/E_a is near unity. Maximal energetic efficiency occurs when E_{es}/E_a approximates 2.0. In patients with heart failure, the left ventricle and the arterial system are suboptimally coupled (E_{es}/E_a becomes less than unity). Beta-blockade improves this situation.[20] In patients with myocardial infarction, suboptimal coupling ratio is associated with poor prognosis over the next 5 years.[29] S_m as a measure of the status of ventricular-arterial coupling may allow accurate evaluations of cardiovascular pathophysiology and also predictions of prognosis in patients with cardiac disease. The ventricular-arterial coupling ratio can be predicted also by LVEF.[8] However, LVEF assessment requires precise definition of the endocardial borders on conventional echocardiography, which is complicated by trabeculae or endocardial dropout. Precise endocardial definition is sometimes difficult, especially in obese patients, the elderly, and patients with pulmonary disease. Recording of mitral annular motion has the advantage that it is not dependent on the endocardial definition and is therefore relatively independent of image quality.[7] S_m measurement can be an alternative to LVEF assessment to predict the status of ventricular-arterial coupling in such patients.

Study Limitations

In accordance with a previous canine study,[17] sonomicrometry consistently underestimated systolic mitral annular velocity compared with TD echocardiography (Figure 2D). This discrepancy may be attributed to the location of the crystals, which are implanted in the subepicardium. Although longitudinally directed myocardial fibers in both subendocardial and subepicardial layers of the left ventricle may play a major role in the magnitude of systolic mitral annular velocity,[1] systolic shortening of subepicardial fiber is significantly smaller than that of subendocardial fiber.[30] In humans, the absolute value of mitral annular velocity measured by TD echocardiography agreed with that measured by cardiac magnetic resonance imaging, which is the widely accepted gold standard for the assessment of LVV and function.[31] Although sonomicrometry is useful in animal experiments

for the assessment of heart motion, our data suggest that S_m obtained by sonomicrometry in this study might have underestimated the true LV longitudinal shortening velocity. However, a strong correlation was observed between S_m and S_{mTD} (Figure 2D). Percentage changes in S_m and S_{mTD} were also correlated tightly (Figure 2E), indicating that S_m sensitively tracked changes in S_{mTD}. Taken together, it is fair to say that conclusions provided by sonomicrometry in this study are comparable, at least qualitatively, with those obtained by TD echocardiography.

In analyzing the experimental data, we relied on E_{es}' (the P_{es}/V_{es} ratio) to quantify LV contractility, which can be evaluated more precisely by both the slope (E_{es}) and volume axis intercept (V_0) of the relationship between P_{es} and V_{es} (Figure 1A).[12] It was unclear how each contributed to the magnitude of S_m in this study. Despite these limitations, the P_{es}/V_{es} ratio as a single contractile index simplifies the statistical analysis of contractility.[9,20]

Colinearity among the cardiovascular parameters as noted between E_{es}' and $V_{ed}^{1/3}$ might have affected the present results. The colinearity may be attributable to the nature of the protocols, such as heart failure induction, which depresses LV contractility and increases preload simultaneously. However, the protocols are analogous to commonly observed clinical setting or practice, that is, relevant to possible clinical application of the conclusions of this study.

CONCLUSIONS

LV contractility and afterload independently determine S_m. The effects of LV preload and EJT on S_m might be small, even though they are theoretically associated with S_m. S_m strongly reflects the status of ventricular-arterial coupling.

REFERENCES

1. Nikitin NP, Witte KK, Thackray SD, de Silva R, Clark AL, Cleland JG. Longitudinal ventricular function: normal values of atrioventricular annular and myocardial velocities measured with quantitative two-dimensional color Doppler tissue imaging. J Am Soc Echocardiogr 2003;16:906-21.
2. Gulati VK, Katz WE, Follansbee WP, Gorcsan J III. Mitral annular descent velocity by tissue Doppler echocardiography as an index of global left ventricular function. Am J Cardiol 1996;77:979-84.
3. Hori Y, Sato S, Hoshi F, Higuchi S. Assessment of longitudinal tissue Doppler imaging of the left ventricular septum and free wall as an indicator of left ventricular systolic function in dogs. Am J Vet Res 2007;68:1051-7.
4. Mogelvang R, Goetze JP, Pedersen SA, Olsen NT, Marott JL, Schnohr P, et al. Preclinical systolic and diastolic dysfunction assessed by tissue Doppler imaging is associated with elevated plasma pro-B-type natriuretic peptide concentrations. J Card Fail 2009;15:489-95.
5. Nikitin NP, Loh PH, Silva R, Ghosh J, Khaleva OY, Goode K, et al. Prognostic value of systolic mitral annular velocity measured with Doppler tissue imaging in patients with chronic heart failure caused by left ventricular systolic dysfunction. Heart 2006;92:775-9.
6. Mogelvang R, Sogaard P, Pedersen SA, Olsen NT, Marott JL, Schnohr P, et al. Cardiac dysfunction assessed by echocardiographic tissue Doppler imaging is an independent predictor of mortality in the general population. Circulation 2009;119:2679-85.
7. Seo JS, Kim DH, Kim WJ, Song JM, Kang DH, Song JK. Peak systolic velocity of mitral annular longitudinal movement measured by pulsed tissue Doppler imaging as an index of global left ventricular contractility. Am J Physiol Heart Circ Physiol 2010;298:H1608-15.
8. Kass DA, Maughan WL, Guo ZM, Kono A, Sunagawa K, Sagawa K. Comparative influence of load versus inotropic states on indexes of ventricular contractility: experimental and theoretical analysis based on pressure-volume relationships. Circulation 1987;76:1422-36.
9. Borlaug BA, Melenovsky V, Redfield MM, Kessler K, Chang HJ, Abraham TP, et al. Impact of arterial load and loading sequence on left ventricular tissue velocities in humans. J Am Coll Cardiol 2007;50:1570-7.
10. Henein MY, Das SK, O'Sullivan C, Kakkar VV, Gillbe CE, Gibson DG. Effect of acute alterations in afterload on left ventricular function in patients with combined coronary artery and peripheral vascular disease. Heart 1996;75:151-8.
11. Amà R, Segers P, Roosens C, Claessens T, Verdonck P, Poelaert J. The effects of load on systolic mitral annular velocity by tissue Doppler imaging. Anesth Analg 2004;99:332-8.
12. Burkhoff D, Mirsky I, Suga H. Assessment of systolic and diastolic ventricular properties via pressure-volume analysis: a guide for clinical, translational, and basic researchers. Am J Physiol Heart Circ Physiol 2005;289:H501-12.
13. Sunagawa K, Maughan WL, Burkhoff D, Sagawa K. Left ventricular interaction with arterial load studied in isolated canine ventricle. Am J Physiol Heart Circ Physiol 1983;245:H773-80.
14. Hayashi K, Shigemi K, Shishido T, Sugimachi M, Sunagawa K. Single-beat estimation of ventricular end-systolic elastance-effective arterial elastance as an index of ventricular mechanoenergetic performance. Anesthesiology 2000;92:1769-76.
15. Shishido T, Hayashi K, Shigemi K, Sato T, Sugimachi M, Sunagawa K. Single-beat estimation of end-systolic elastance using bilinearly approximated time-varying elastance curve. Circulation 2000;102:1983-9.
16. National Institutes of Health. Guide for the care and use of laboratory animals (NIH Publication No. 85-23). Bethesda, MD: National Institutes of Health; 1996.
17. Opdahl A, Remme EW, Helle-Valle T, Lyseggen E, Vartdal T, Pettersen E, et al. Determinants of left ventricular early-diastolic lengthening velocity: independent contributions from left ventricular relaxation, restoring forces, and lengthening load. Circulation 2009;119:2578-86.
18. Ratcliffe MB, Gupta KB, Streicher JT, Savage EB, Bogen DK, Edmunds LH Jr. Use of sonomicrometry and multidimensional scaling to determine the three-dimensional coordinates of multiple cardiac locations: feasibility and initial implementation. IEEE Trans Biomed Eng 1995;42:587-98.
19. Rankin JS, McHale PA, Arentzen CE, Ling D, Greenfield JC Jr., Anderson RW. The three-dimensional dynamic geometry of the left ventricle in the conscious dog. Circ Res 1976;39:304-13.
20. Maurer MS, Sackner-Bernstein JD, El-Khoury Rumbarger L, Yushak M, King DL, Burkhoff D. Mechanisms underlying improvements in ejection fraction with carvedilol in heart failure. Circ Heart Fail 2009;2:189-96.
21. Colin P, Ghaleb B, Monnet X, Hittinger L, Berdeaux A. Effect of graded heart rate reduction with ivabradine on myocardial oxygen consumption and diastolic time in exercising dogs. J Pharmacol Exp Ther 2004;308:236-40.
22. Fitzmaurice GM, Ravichandran C. A primer in longitudinal data analysis. Circulation 2008;118:2005-10.
23. Odland HH, Kro GA, Munkeby BH, Edvardsen T, Saugstad OD, Thaulow E. Ejection time-corrected systolic velocity improves accuracy in the evaluation of myocardial dysfunction: a study in piglets. Pediatr Cardiol 2010;31:1070-8.
24. Oki T, Fukuda K, Tabata T, Mishiro Y, Yamada H, Abe M, et al. Effect of an acute increase in afterload on left ventricular regional wall motion velocity in healthy subjects. J Am Soc Echocardiogr 1999;12:476-83.
25. Palmieri V, Russo C, Arezzi E, Pezzullo S, Sabatella M, Minichiello S, et al. Relations of longitudinal left ventricular systolic function to left ventricular mass, load, and Doppler stroke volume. Eur J Echocardiogr 2006;7:348-55.
26. Pelà G, Regolisti G, Coghi P, Cabassi A, Basile A, Cavatorta A, et al. Effects of the reduction of preload on left and right ventricular myocardial velocities analyzed by Doppler tissue echocardiography in healthy subjects. Eur J Echocardiogr 2004;5:262-71.

27. Jones CJ, Raposo L, Gibson DG. Functional importance of the long axis dynamics of the human left ventricle. Br Heart J 1990;63:215-20.
28. Burkhoff D, Sagawa K. Ventricular efficiency predicted by an analytical model. Am J Physiol 1986;250:R1021-7.
29. Antonini-Canterin F, Enache R, Popescu BA, Popescu AC, Ginghina C, Leiballi E, et al. Prognostic value of ventricular-arterial coupling and B-type natriuretic peptide in patients after myocardial infarction: a five-year follow-up study. J Am Soc Echocardiogr 2009;22:1239-45.
30. Sabbah HN, Marzilli M, Stein PD. The relative role of subendocardium and subepicardium in left ventricular mechanics. Am J Physiol 1981;240:H920-6.
31. Marsan NA, Westenberg JJ, Tops LF, Ypenburg C, Holman ER, Reiber JH, et al. Comparison between tissue Doppler imaging and velocity-encoded magnetic resonance imaging for measurement of myocardial velocities, assessment of left ventricular dyssynchrony, and estimation of left ventricular filling pressures in patients with ischemic cardiomyopathy. Am J Cardiol 2008;102:1366-72.

APPENDIX

Instantaneous LVP, P(*t*), and LVV, V(*t*), are related by the following formula:

$$V(t) = \frac{P(t)}{E(t)} + V_0, \tag{A2}$$

where E(*t*) is time-varying LV elastance and V_0 is the volume axis intercept of the relationship between P_{es} and V_{es}.[12] S_m is a parameter of the ejection phase. The left ventricle has an ellipsoid shape, and the ratio of LV longitudinal length, L(*t*), to short-axis length is assumed to be constant during the ejection phase. L(*t*) and its time derivative are expressed as follows:

$$L(t) = \alpha[V(t)]^{1/3}, \tag{A3}$$

$$dL(t)/dt = \frac{\alpha}{3} \cdot dV(t)/dt \cdot [V(t)]^{-2/3}. \tag{A4}$$

During the ejection phase, because P(*t*) can be approximated to P_{es} (Figure 1A), equation A2 is rewritten as follows:

$$V(t) = \frac{P_{es}}{E(t)} + V_0. \tag{A5}$$

Differentiation of both sides of equation A5 with respect to time yields

$$dV(t)/dt = \frac{-P_{es} \cdot dE(t)/dt}{[E(t)]^2}. \tag{A6}$$

During the ejection phase, because E(*t*) increases linearly with respect to time,[14,15] dE(*t*)/dt is expressed as follows (Figure 1B):

$$dE(t)/dt = \frac{E_{es} - E_{ad}}{EJT}, \tag{A7}$$

where E_{ad} is the elastance value at the end of the isovolumic contraction phase (Figure 1B).[14,15] Substituting equation A7 into equation A6 yields

$$dV(t)/dt = \frac{-P_{es}}{[E(t)]^2 \cdot EJT} \cdot (E_{es} - E_{ad}). \tag{A8}$$

Substituting equations A5 and A8 into equation A4 yields

$$dL(t)/dt = \frac{-\alpha}{3} \cdot \frac{P_{es}}{EJT} \cdot (E_{es} - E_{ad}) \cdot \frac{1}{[E(t)]^{4/3}} \cdot \left(\frac{1}{P_{es} + V_0 \cdot E(t)}\right)^{2/3}. \tag{A9}$$

Peak shortening velocity of LV longitudinal length, S_m, corresponds to the absolute value of peak negative dL(*t*)/dt during the ejection phase. Because E(*t*) increases constantly during this period (Figure 1B), dL(*t*)/dt assumes its peak negative value when E(*t*) is E_{ad}. Hence, S_m can be expressed as follows:

$$S_m = \frac{\alpha}{3} \cdot \frac{P_{es}}{EJT} \cdot (E_{es} - E_{ad}) \cdot \frac{1}{E_{ad}^{4/3}} \cdot \left(\frac{1}{P_{es} + V_0 \cdot E_{ad}}\right)^{2/3}. \tag{A10}$$

As shown in Figure 1A, E_{es}, E_{ad}, and E_a will be approximated by P_{es}, V_{es}, V_{ed}, and V_0 as follows:

$$E_{es} = \frac{P_{es}}{V_{es} - V_0}, \tag{A11}$$

$$E_{ad} = \frac{P_{es}}{V_{ed} - V_0}, \tag{A12}$$

$$E_a = \frac{P_{es}}{V_{ed} - V_{es}}. \tag{A13}$$

Substituting V_{es} in equation A11 and V_{ed} in equation A12 into equation A13 yields

$$E_{es} - E_{ad} = \frac{E_{es} \cdot E_{ad}}{E_a}. \tag{A14}$$

Substituting $(E_{es} - E_{ad})$ in equation A14 into equation A10 yields

$$S_m = \frac{\alpha}{3} \cdot \frac{P_{es}}{EJT} \cdot \frac{E_{es}}{E_a} \cdot \frac{1}{E_{ad}^{1/3}} \cdot \left(\frac{1}{P_{es} + V_0 \cdot E_{ad}}\right)^{2/3}. \tag{A15}$$

Substituting E_{ad} in equation A12 into equation A15 yields

$$S_m = \frac{\alpha}{3} \cdot \frac{E_{es}}{E_a} \cdot \frac{V_{ed}^{1/3}}{EJT} \cdot \left(1 - \frac{V_0}{V_{ed}}\right). \tag{A16}$$

If we assume that $V_{ed} \gg V_0$, equation A16 is rewritten as

$$S_m = \frac{\alpha}{3} \cdot \frac{E_{es}}{E_a} \cdot \frac{V_{ed}^{1/3}}{EJT},$$

which is equation 1 shown in the "Methods" section.